ADVANCED FUNCTIONAL MATERIALS

Supporting Information

for *Adv. Funct. Mater.*, DOI 10.1002/adfm.202307590

Hierarchical Weaving Metafabric for Unidirectional Water Transportation and Evaporative Cooling

Ling Zhang, Yuwei Guo, Ruolian Mo, Xiang Liu, Guang Wang, Ronghui Wu and Hongling Liu**

Supporting information

Hierarchical weaving metafabric for unidirectional water transportation and evaporative cooling

Ling Zhang[1], *Yuwei Guo*[1], *Xiang Liu*[1], *Guang Wang*[1], *Ronghui Wu*[1,2*],*Hongling Liu*[1*]

L. Z., Y.G., R.M., X.L., G. W., Dr. R. W., Prof. H. L.

Key Laboratory of Textile Science &Technology, Ministry of Education, College of Textiles, Donghua University, Shanghai 201620, China.

Email: hlliu@dhu.edu.cn

Dr. R. W.

Pritzker School of Molecular Engineer, University of Chicago, Chicago, 60637, USA.

Email: ronghuiwu@uchicago.edu

Keywords: unidirectional water transportation, weaving metafabric, evaporative cooling, asymmetric wettability, superhydrophobicity

Figure S1. SGA598 semi-automatic loom for continuous UWTM weaving.

Figure S2. An optical photo of a weft-double-weave fabric.

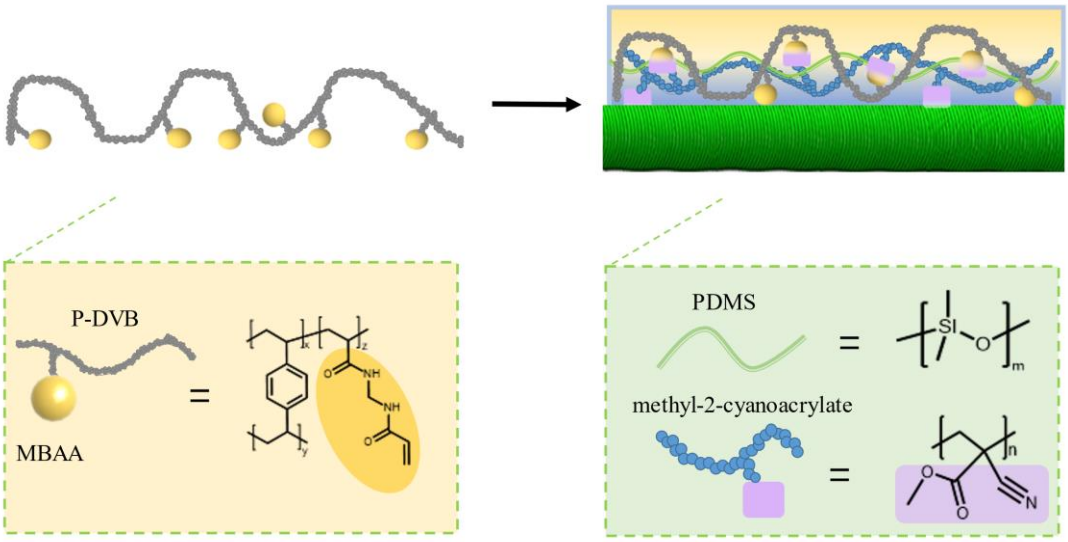

Figure S3. Synthesis mechanism of co-MBAA-DVB coating polyester yarn.

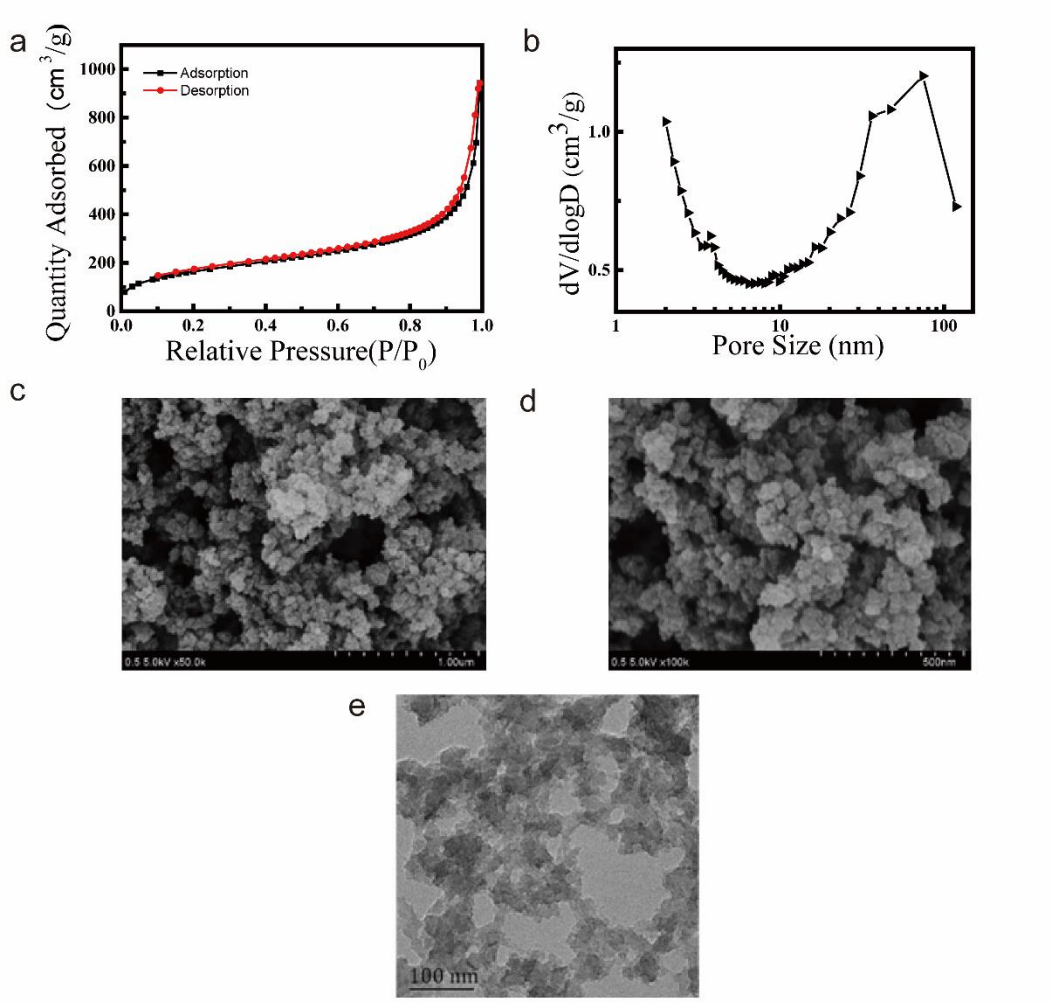

Figure S4. Structural characterization of the nanoporous polymer. (a) The property of obtained powders was studied using nitrogen-sorption isotherm, which was collected at 77K. The BET surface area of nano-polymers was calculated to be as high as 604.14 m^2g^{-1}, suggesting that the existence of rich pore structure. The nitrogen uptake still increases at high relative pressure of 0.8~1.0, demonstrating the presence of macropores (>50 nm); (b) The average pore width of the sample was 96.5nm; (c) and (d) are the SEM image which indicate the presence of multi-scale nanoparticles. (e) TEM image further verified the porous structures.

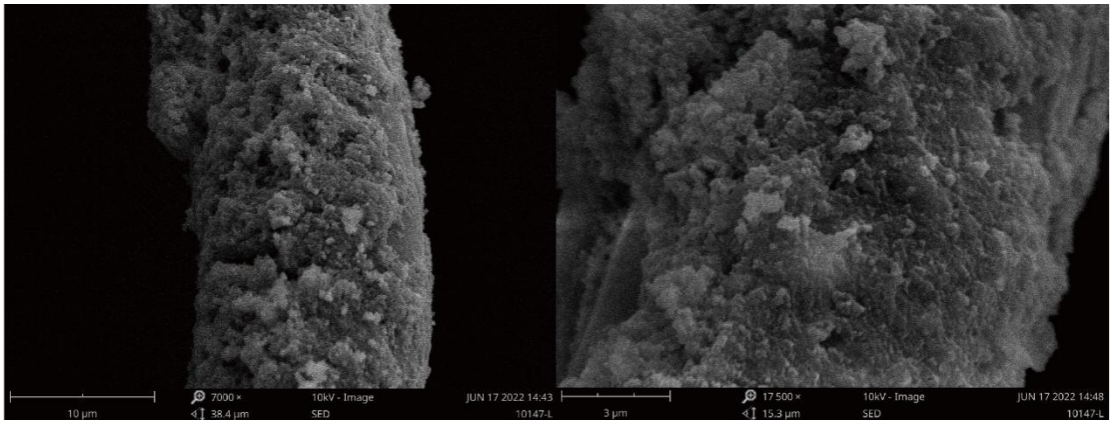

Figure S5. SEM images of random selected regions on SIWY.

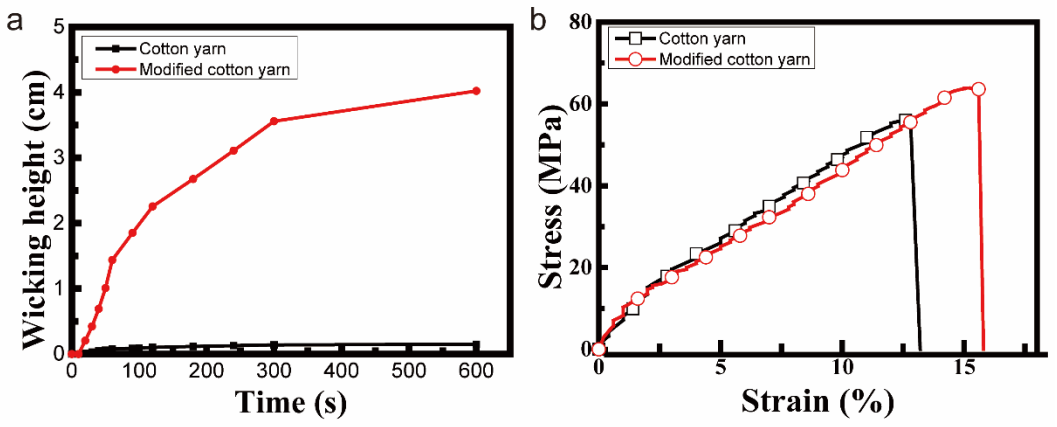

Figure S6. (a) Wicking height and (b) mechanical performance of the cotton yarns and modified cotton yarns.

Table S1. Fabric structure and process setting of 6 samples

Sample	Fabric weave	Warp	Weft		Weft density [yarns/10cm]	Thickness/[mm]
			Hydrophilic surface	Hydrophobic surface		
3#	Weft-backed-weave	Polyester A	Viscose	Polyester B	432	1.09
4#	Weft-backed-weave	Polyester A	Cotton	Polyester B	424	1.21
1#	Satin-weave	Polyester B	Viscose		616	0.98
2#	Satin-weave	Polyester B	Cotton		602	1.18
5#	Stitching-double-weave	Polyester A	Viscose	Polyester B	464	0.96
6#	Stitching-double-weave	Polyester A	Cotton	Polyester B	444	1.10

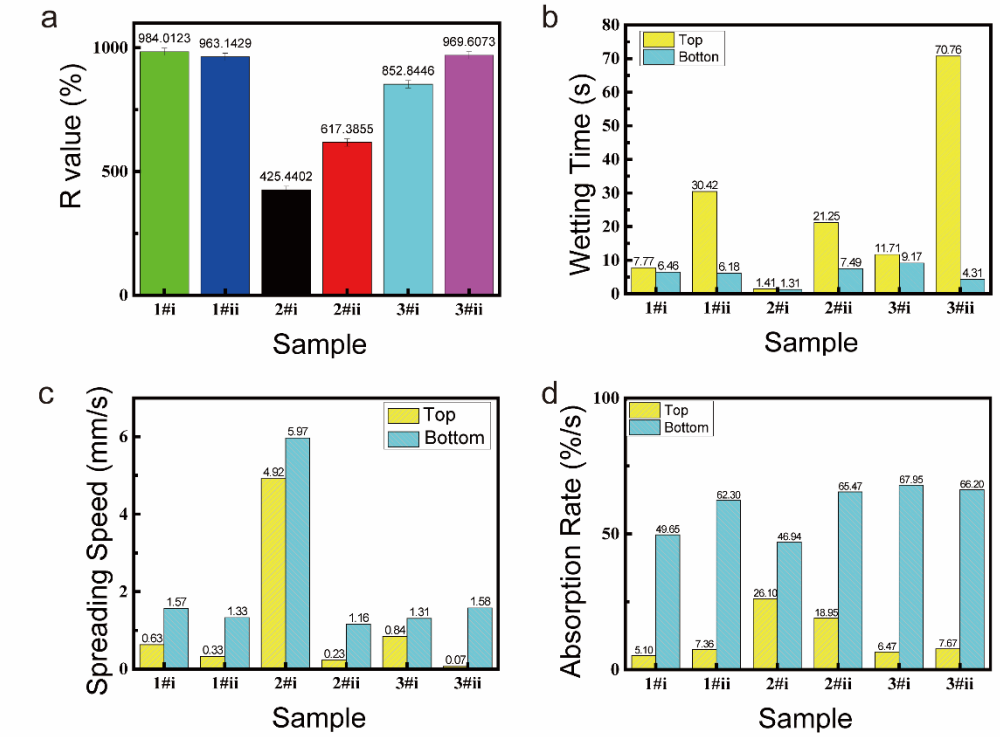

Figure S7. MMT test results of fabrics. (a) accumulative one-way transport Capacity (b)Wetting time top/bottom; (c)spreading speed top/bottom; (d) absorption rate top/bottom.

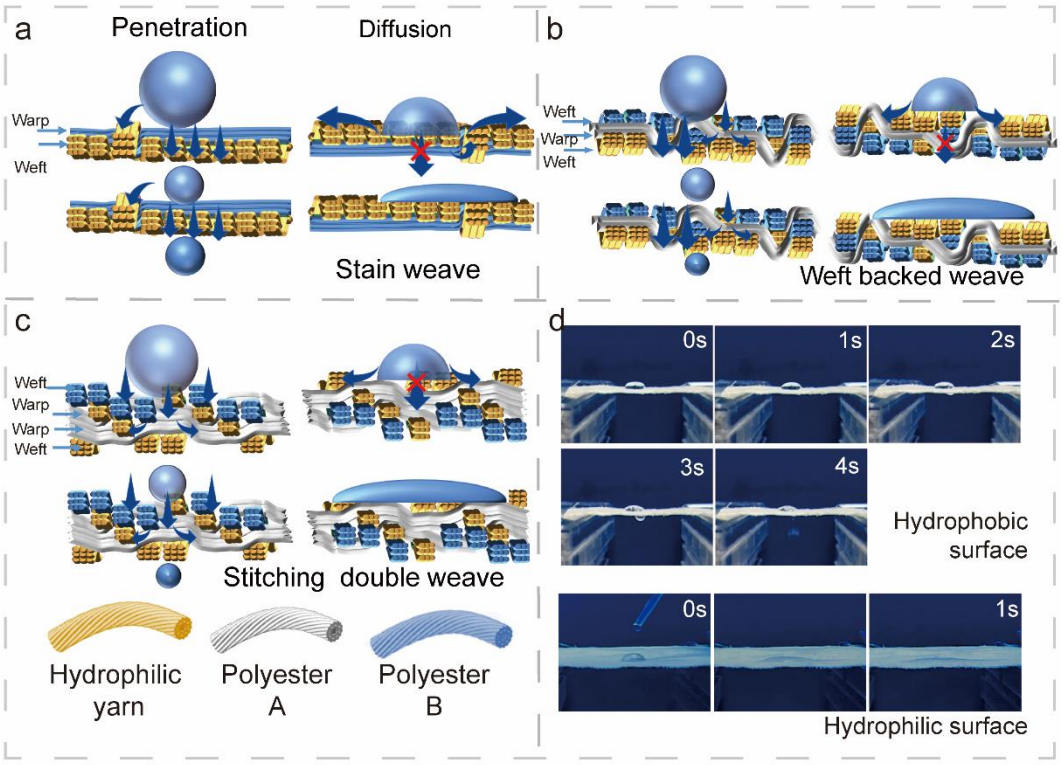

Figure S8. Liquid penetration and diffusion mechanism and experiment of UWTM with different wettability and microstructure. (a-c) Liquid penetration and diffusion mechanism of (a)stain weave, (b)weft backed weave and (c)stitching double weave. (d-e) Photographs of (d) penetration process of 2μl droplets on 3# hydrophobic surface and (e) diffusion process of hydrophilic surface.

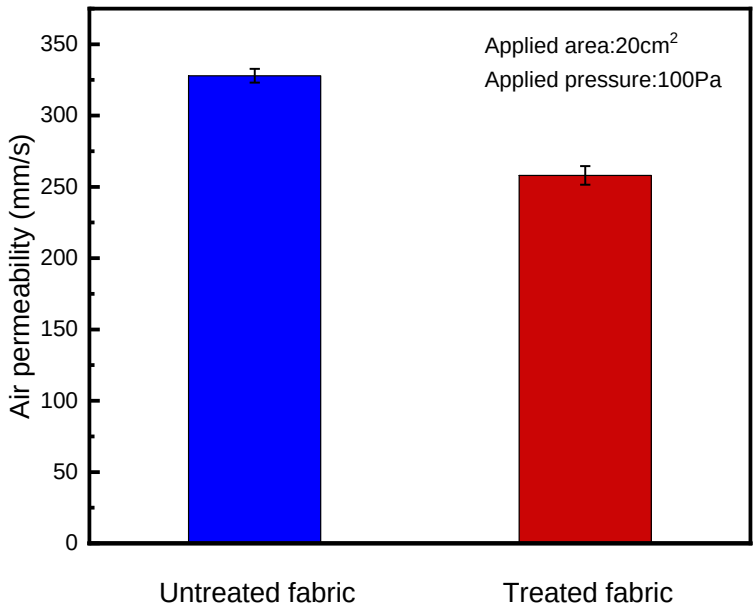

Figure S9 Comparison of air permeability of weft-double-weave fabrics with and without superhydrophobic treatment.

The air permeability of fabric is a key index to evaluate the comfort degree of functional textiles. Therefore, we supplemented the air permeability comparison experiment of untreated and treated polyester and viscose yarns interwoven fabrics, the test standard based on GBT5453-1997 textile fabric breathability determination. As shown in Figure S8, compared to pristine fabrics (327.93mm^{-1}), weft-double-weave fabrics (1#) are also capable of demonstrating good air permeability (258.07mm^{-1}). The slight decrease in the air permeability of the treated fabric was mainly caused by the obstruction of the fabric pores caused by the co-MBAA-DVB nanoparticles attached to the surface of the hydrophobic polyester yarns, which resulted in the disappearance of some tiny pores between the yarns. This result shows that the unidirectional water transportation fabric still exhibits good breathability and comfort in wearable application areas. The combination of proper air permeability and excellent unidirectional water-transportation will greatly extend the range of applications of versatile textiles.

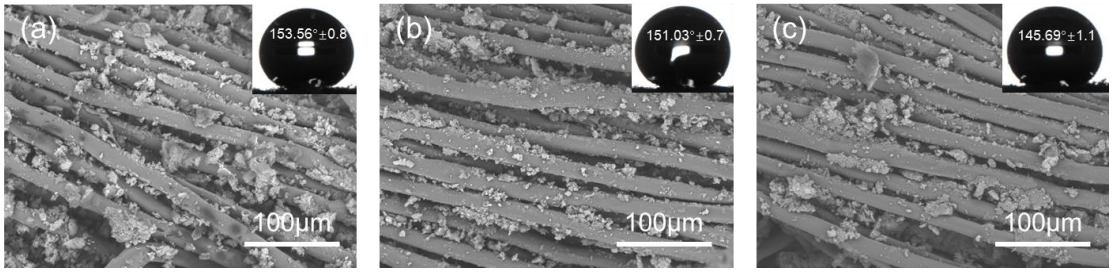

Figure S10 SEM photos of the treated fabric after 1 and 5 washing cycles. (a) Unwashed weft-double-weave fabric, (b) 1 washing cycle, (c) 5 washing cycles.

As shown in Figure S9, after 1 washing cycle, the adhesion of co-MBAA-DVB on the fabric surface does not decrease significantly, which can also be seen from its surface wettability, and the fabric still has the feature of superhydrophobic (WCA is 151.03°). After 5 washing cycles, the adhesion of co-MBAA-DVB on the fabric surface decreased gradually with the increase of washing times, but they are still evenly distributed on the yarns, giving the yarns a certain roughness, resulting in a hydrophobic effect of the fabric (WCA is 145.69°), and forming a Janus wettability gradient with the hydrophilic side. Therefore, the unidirectional water transfer characteristics of UWTM are potentially stable after different washing cycles.

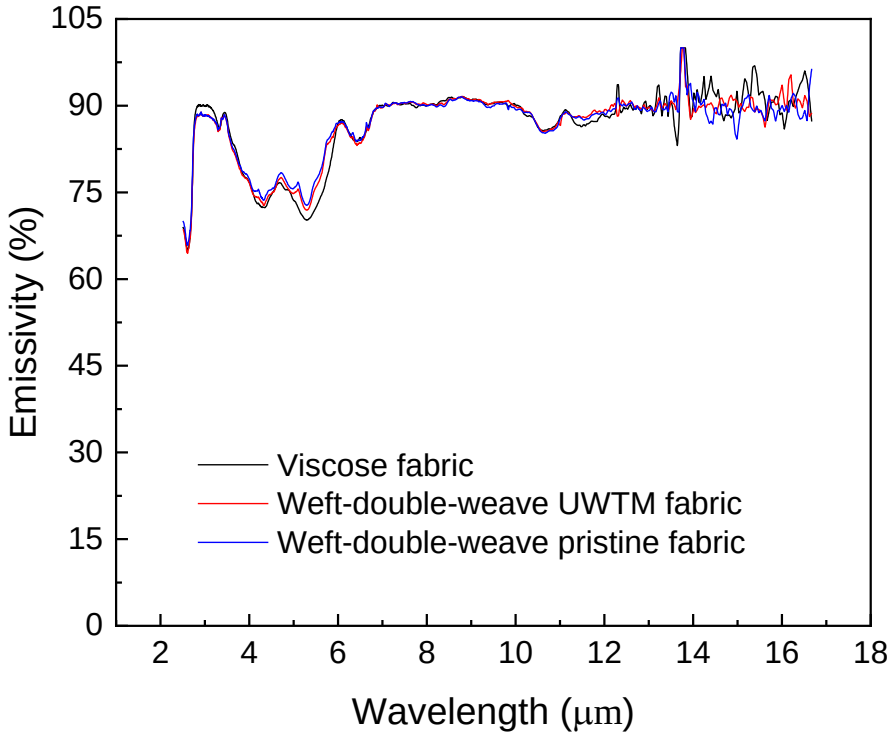

Figure S11. MIR emissivity of viscose fabric, pristine weft-double-weave fabric, and weft-double-weave UWTM fabric surface.

REFERENCES

[1] J. A. Rippon, J. Soc. Dyers Col . **1984**, 100, 298.